Energy Proceedings
Vol 36, 2023
ISSN 2004-2965

Iron-Based Oxygen Carrier Particles With High Performance for Mid-Temperature Chemical Looping Methane Reforming

Yang Li[1,2], Mingkai Liu[1], Jinrui Zhang[1,2], Tianlong Yang[1,3], Qiong Rao[1,2], Zhongrui Gai[1,3], Ying Pan[1*]
1 Institute of Engineering Thermophysics, Chinese Academy of Sciences, 11 Beisihuanxi Rd., Beijing 100190, P. R. China
2 University of Chinese Academy of Sciences, No.19A Yuquan Rd., Beijing 100049, P. R. China
3 International Research Center for Renewable Energy & State Key Laboratory of Multiphase Flow in Power Engineering, Xi'an Jiaotong University, 710049, China
(*Corresponding Author: panying@iet.cn)

ABSTRACT

Hydrogen is an ideal and potential energy carrier due to its high energy efficiency and low pollution. An alternative and promising approach to hydrogen generation is the chemical looping steam methane reforming (CL-SMR) over iron-based oxygen carriers. However, the process faces challenges such as high reaction temperature (>850°C) and low methane conversion. We demonstrate that Ni-mixed Fe-based oxygen carrier particles have significantly improved the methane conversion and hydrogen production rate in the range of 450-600°C under atmospheric pressure. The effect on the reaction reactivity of oxygen carrier particles with different Ni-based particles mixed mass ratios has been determined in the continuous unit. More than 85% of methane conversion has been achieved at 600oC, and hydrogen can be produced in both reduction and oxidation steps. Moreover, the iron-based oxygen carrier particles exhibited good cyclic performance during 150 consecutive redox cycles at 600°C. The mid-temperature iron-based oxygen carrier particles, integrated with a moving-bed chemical looping system, might provide a powerful approach toward more efficient and scalable hydrogen production.

Keywords: chemical looping, hydrogen production, mid-temperature, oxygen carrier particles

NONMENCLATURE

Abbreviations	
CL-SMR	Chemical looping steam methane reforming
SMR	Steam methane reforming

Symbols	
$Con_{i,out}$	Concentration of component *i* in the outlet gas
D_C	Carbon deposition, mmol/g
M_{OC}	Mass of oxygen carrier particles, g
$R_{H\text{-}C}$	Hydrogen to carbon ratio
S_{CO}	CO selectivity
t	Reaction time, min
$V_{i,in}$	Flow rate of component *i* in the inlet gas, mL/min
$V_{i,out}$	Flow rate of component *i* in the outlet gas, mL/min
X_{CH_4}	Methane conversion

1. INTRODUCTION

As climate issues become increasingly prominent, the transformation of energy structure is imminent, and energy fuel carriers with zero carbon emissions are essential. Hydrogen is one of the most promising energy carriers because of its high energy density and the fact that only water vapor is emitted during combustion, which can reduce pollutants and greenhouse gas emissions. The WEO 2020 projects that hydrogen should account for 35% of the energy structure to achieve net zero emissions by 2050 [1]. Steam methane reforming (SMR) is the most mature method of hydrogen production, but it is limited by the reaction equilibrium in the mid-temperature range [2]. Chemical looping steam methane reforming (CL-SMR) is a novel method for hydrogen production [3, 4], which can reduce the temperature of hydrogen production by contrast with SMR. This process involves reduction and oxidation of the looping material-oxygen carrier. The oxygen carrier

This is a paper for the 9th Applied Energy Symposium: Low Carbon Cities and Urban Energy Systems (CUE2023), Sep. 2-7, 2023, Matsue & Tokyo, Japan.

generates syngas and pure hydrogen by circulating between the reduction stage in which reacts with methane to lose lattice oxygen and the oxidation stage in which reacts with water to return to metal oxides.

The design and preparation of oxygen carriers is a key issue in CL-SMR. A series of metal oxides, such as Fe_2O_3, NiO, CuO and perovskite-type oxides as well as their blends have been confirmed to be able to participate in the reaction as oxygen carriers [4-8]. One problem with chemical looping hydrogen production is that there are few large-scale demonstration applications. In addition to system design, low-cost oxygen carriers that can be prepared on a large-scale are also important issues. Fe-based oxides are considered as a promising oxygen carrier due to its wide source, low cost, and non-polluting properties [9]. Because of this, Fe_2O_3 is also commonly used as an oxygen carrier for chemical looping demonstration applications [10-12]. A typical demonstration project is the 250kW_{th} syngas chemical looping system of Ohio State University, which uses a moving bed to realize the circular flow of iron-based oxygen carriers [13].

However, Fe-based oxygen carriers suffer from the challenge of high reaction temperatures for achieving good performance, often requiring temperatures above 800°C [14, 15]. This issue greatly hinders the widespread use of Fe-based oxygen carriers. The situation was first illustrated through thermodynamic analysis by Steinfeld et al [16]. To address this issue, the reaction performance with methane is usually improved by regulating the oxygen carrier through doping [7, 8, 17]. For instance, Ni-doping is a key method of regulating oxygen carrier performance, as the reactivity of NiO and CH_4 at low temperatures is particularly remarkable [18].

In our study, to ensure the mechanical properties of the oxygen carrier particles, we subjected them to calcination at 1050°C, thus enabling their potential application in fluidized bed or moving bed systems. Different mixing mass ratios and variable temperature performance were studied by continuous operation in a CL-SMR process. To determine the cycle stability of the formed particles, multiple cycles were performed on a fixed bed reactor, and we conducted characteristic of the samples. We have successfully achieved high hydrogen production and performance in CL-SMR at mid-temperature by utilizing a mixture of 20 wt% Ni-doped Fe-based oxygen carrier particles and Ni-based oxygen carrier particles. Our work provides a promising method for large-scale oxygen carrier particle fabrication for CL-SMR at middle temperature.

2. MATERIAL AND METHODS

2.1 Sample preparation

All oxygen carrier particles used in this work are prepared by mechanical mixing method. Alumina oxide (Macklin AR) as an inert carrier, Iron oxide (II, III) (Macklin 99%) and NiO/Al_2O_3 powders prepared in previous work [19] are mixed according to the mass ratio of metal oxide and inert carrier mass ratio is 6:4. The mixed oxygen carrier powder is mixed with kaolin and cellulose according to the mass ratio of 1:0.06:0.1. The mixed powder added with deionized water was granulated by an extruder (Xinyite Shenzhen) with a diameter of 2 mm and a roller (Xinyite Shenzhen) to obtain 2 mm diameter oxygen carrier particles. Obtained particles was then calcinated under ambient air at 1323 K for 6 h. Finally, the resultant particles were named as Fe-P in which the mass ratio of NiO and Fe_2O_3 is 1:5 and Ni-P which is prepared without iron oxide (II,III) added.

2.2 Characterization

The crushing strength of the oxygen carrier particles was measured by using a crushing testing machine (Siwei Shanghai). This measurement was repeated more than 10 times to obtain the average mechanical strength of the particles. The BET surface area of the oxygen carrier particles was measured by the nitrogen absorption method in a Micromeritics ASAP 2020 instrument.

The identification of crystalline phases was performed by X-ray Diffraction (D8 focus, Bruker) using Cu Kα radiation operated at 40 kV and 40 mA. For XRD analysis, the samples were scanning with a 2θ range of 10-90° at a speed of 12°/min.

2.3 Experiment setup and test procedure

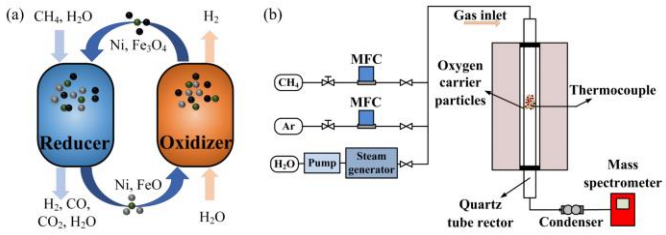

Fig. 1. Schematic diagram of (a) CL-SMR reaction, (b) experimental setup.

2.3.1 Chemical looping reactions

The schematic diagrams of the chemical looping reaction and facility are shown in Fig. 1. The detail apparatus can be found in our previous study [19]. In the case of the isothermal experiment, the particles with a total mass of 0.4 g, of which the mass ratio of Ni-P and Fe-P is 1:3 are used as oxygen carriers. To activate oxygen

carrier particles, the particles were reduced by hydrogen (12 mL/min Argon and 2 mL/min Hydrogen) for 20 minutes before redox cycles. The oxygen carrier particles were then oxidized by H_2O (2 μL/min) at Ar atmosphere for 20 minutes to return to the chemical looping cycle state. The redox experimental procedure involves the following steps: (1) the particles were reduced by methane (CH_4 1 mL/min, H_2O 1 μL/min, and Ar 6 mL/min) for 10 min; (2) the oxidation step was performed by water (μL /min) diluted in Ar (6 mL/min) for 8 minutes. (3) To avoid mixing of the reduction and oxidation stage gas, a purge gas flow of Ar was introduced for about 8 min or more before the switch between the reducing gas and oxidizing gas. An online mass spectrometer (Pfeiffer Omnistar GSD 320) was used to monitor the concentration of outlet gas continuously during the reaction.

2.3.2 Thermogravimetric analysis

The cyclic stability of oxygen carrier particles can be tested by the repetitive weight changes of oxygen gain and loss. The mass loss of the oxygen carrier particles in redox cycles was examined in a thermogravimetric analyzer (DTG-60H, SHIMADZU) at 600°C. About 40 mg of Fe-P were placed in an alumina crucible and heated from ambient temperature to selected temperature under pure Ar gas flow. Methane reduction was set for 5 min in the reduction stage, air oxidation was set for 4 min in the oxidation stage, and pure N_2 flow was used to purge the thermogravimetric reaction chamber in the gas switching phase. It's worth noting that to avoid the excessive loose particles' structure due to excessive temperature change, the temperature rising or cooling rates were kept at 10°C/min.

2.3.3 Conversion and reaction rate calculation

The volume of the outlet gas can be obtained by integrating the mass spectrum, taking methane as an example:

$$V_{\mathrm{CH_4},out} = \frac{Con_{\mathrm{CH_4},out}}{Con_{\mathrm{Ar},out}} \bullet V_{\mathrm{Ar},in} \tag{1}$$

Where $V_{\mathrm{CH_4},out}$ is the instantaneous volumetric rate of methane in the outlet gas, $Con_{\mathrm{CH_4},out}$ and $Con_{\mathrm{Ar},out}$ is the concentration ratio of methane and Argon detected by mass spectrometry in the outlet gas, $V_{\mathrm{Ar},in}$ is the volumetric rate of Argon.

Based on the above gas volume conversion method, the methane conversion ($X_{\mathrm{CH_4}}$), CO selectivity (S_{CO}), carbon deposition (D_{C}) calculated by carbon balance and H-C molar ratio ($R_{\mathrm{H-C}}$) during the reduction reaction were calculated by the following formula:

$$X_{\mathrm{CH_4}} = \frac{\int_0^t V_{\mathrm{CH_4},\mathrm{in}}\mathrm{d}t - \int_0^t V_{\mathrm{CH_4},out}\mathrm{d}t}{\int_0^t V_{\mathrm{CH_4},\mathrm{in}}\mathrm{d}t} \tag{2}$$

$$S_{\mathrm{CO}} = \frac{\int_0^t V_{\mathrm{CO},out}\mathrm{d}t}{\int_0^t V_{\mathrm{CO},out}\mathrm{d}t + \int_0^t V_{\mathrm{CO_2},out}\mathrm{d}t} \tag{3}$$

$$D_{\mathrm{C}} = \frac{\int_0^t V_{\mathrm{CH_4},in}\mathrm{d}t - \int_0^t V_{\mathrm{CH_4},out}\mathrm{d}t - \int_0^t V_{\mathrm{CO},out}\mathrm{d}t - \int_0^t V_{\mathrm{CO_2},out}\mathrm{d}t}{V_m \bullet M_{OC}} \tag{4}$$

$$R_{\mathrm{H\text{-}C}} = \frac{\int_0^t V_{\mathrm{H_2},out}\mathrm{d}t}{\int_0^t V_{\mathrm{CO},out}\mathrm{d}t + \int_0^t V_{\mathrm{CO_2},out}\mathrm{d}t} \tag{5}$$

where V_m is the molar volume of gas, M_{OC} is the mass of the oxygen carrier particles.

3. RESULTS AND DISCUSSION

3.1 Sample characterization

Table 1 shows the physical characteristics of the fresh oxygen carrier particles and cycled oxygen carrier particles. The particles calcined at 1050°C have excellent mechanical strength, which gives the particles a good potential to be suitable for moving bed reactor or fluidized bed reactor and can effectively prevent fragmentation and attrition of particles which is the largest cost in chemical looping reaction after multiple cycles.

Table 1. Physical properties of oxygen carrier particles.

Particles	Crushing strength (N)	BET surface area (m^2/g)	Pore volume (cm^3/g)
Fresh	13.44	6.84	0.0238
Reaction cycled	13.25	6.74	0.0251
TGA cycled	11.14	10.72	0.0645

Figure 2a shows the distribution histogram of the crushing strength of different particles, after several chemical looping cycles, the crushing strength of the particles decreased slightly. Although the crushing strength of the thermogravimetric test samples (more than 150 cycles) decreased by nearly 20%, they still had acceptable mechanical strength, higher than the 5~10 N mentioned in other literature [20, 21]. As the number of

cycles increases, the BET surface area and pore volume of the particles will increase due to the lattice oxygen transfer of the particles. This is opposite to the development trend of the crushing strength of the particles, but it will have a positive effect on the reaction performance of the particles.

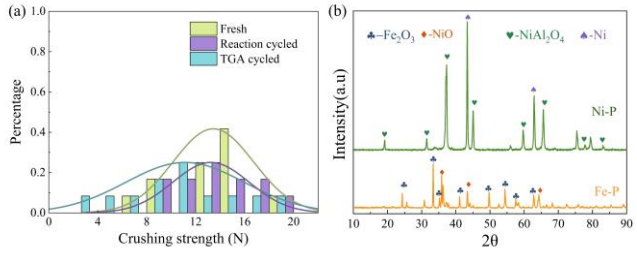

Fig. 2. (a) crushing strength histogram, (b) XRD patterns of Ni-P and Fe-P.

XRD patterns for the fresh particles are shown in Fig. 2b. It can be seen that the formation of $NiAl_2O_4$ in Ni-P after the calcination[22]. The main active components in fresh Fe-P after calcination are NiO and Fe_2O_3, which means that the crystal phase did not change after calcination. Due to the low content of nickel, the expected peak position of $NiAl_2O_4$ in the sample spectrum is not obvious. XRD results indicate that calcination leads to the generation of spinel but does not change the main crystal phase of oxygen carrier particles.

3.2 Fixed-bed reaction test

3.2.1 Selection of oxygen carrier particles

The particles were investigated for methane conversion and hydrogen production by alternating exposure at 600°C to methane, inert gas, and water vapor as described in the experimental procedure. Figure 3a shows the results of separating the original 1:3 mass ratio particles of Ni-based particles and Fe-based particles to judge whether the particle mixing is effective for the methane reaction performance and hydrogen production of the mid-temperature chemical looping reaction. After particle mixing, the CH_4 conversion increased to over 85%. Only the reduction stage hydrogen production is already higher than the sum of the unmixed case, while the oxidation step also provides additional hydrogen production. It shows that the performance of the mixed particles is not the result of the sum of reactivity of individual particles.

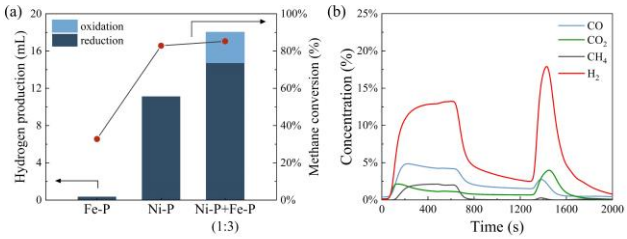

Fig. 3. (a) Performance comparison of particle mixing and non-mixing at 600°C, and (b) mass spectrometer outlet gas concentration diagram of methane steam reforming chemical looping reaction with 1:3 mass ratio of Ni-based and Fe-based particles.

Ni cannot be oxidized back to NiO in the case of a chemical looping reaction in which the reaction gas in the oxidation step is water vapor. Fe-P has a low degree of reaction with methane at 600°C, and the main products are CO_2 and H_2O. In the oxidation stage, particles cannot react with water because the reduction degree cannot reach FeO. The addition of Ni-P in a certain mass ratio reduces the reaction temperature of CH_4 and Fe-based oxygen carrier particles so that part of Fe_3O_4 is reduced to FeO by CH_4 in the reduction step, which usually requires a temperature of more than 800°C. The oxidation step participated by FeO can decompose water to produce hydrogen and restore to the Fe_3O_4. The reaction trend monitored by mass spectrometer is shown in Fig. 3b.

3.2.2 Effect of particles doping ratio

To analyze the effect of the mass ratio of Ni-P added on the reaction performance of the mixed particles, a series of experiments were carried out by changing the mass ratio of Ni-P and Fe-P while keeping the total mass of the oxygen carrier particles constant. As shown in Fig. 4, the mass ratio of Ni-P to Fe-P is 1:1, 1:3, and 1:7 respectively. Under the same working conditions, the mass ratio of Ni-P to Fe-P used in the previous part is 1:3, which is a better mass ratio, and the methane conversion and the hydrogen production in the two steps of reduction and oxidation are both higher. When the proportion of Ni-P is higher, we speculate that the reaction performance with methane in the reduction step may be better, but it will lead to a decrease in the H_2 production in the oxidation step because fewer Fe-based oxygen carriers react with water. The reaction performance of the reduction step decreases when the proportion of Ni-P is lower due to less active components.

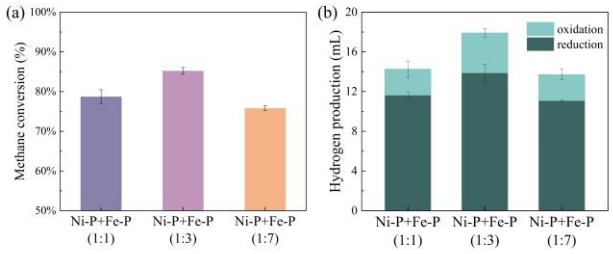

Fig. 4. Reaction performance corresponding to different mixing mass ratios at 600°C, (a) CH_4 conversion and (b) H_2 production.

3.2.3 The oxygen carrier particles behavior

Figure 5 shows the particle's behavior in a continuous redox cycle at 600°C, As shown in Fig. 5a, CH_4 conversion is stable at 85%, and CO selectivity is around 0.5 which means that there is a large proportion of chemical looping combustion in the reduction stage. It is observed that H_2 production in the oxidation step is about 35% of the production in the reduction step in Fig. 5b. Figure 5c shows that the amount of carbon deposition in the reduction stage is precious little due to the water vapor participates in the reaction, and the H-C ratio is close to 3.

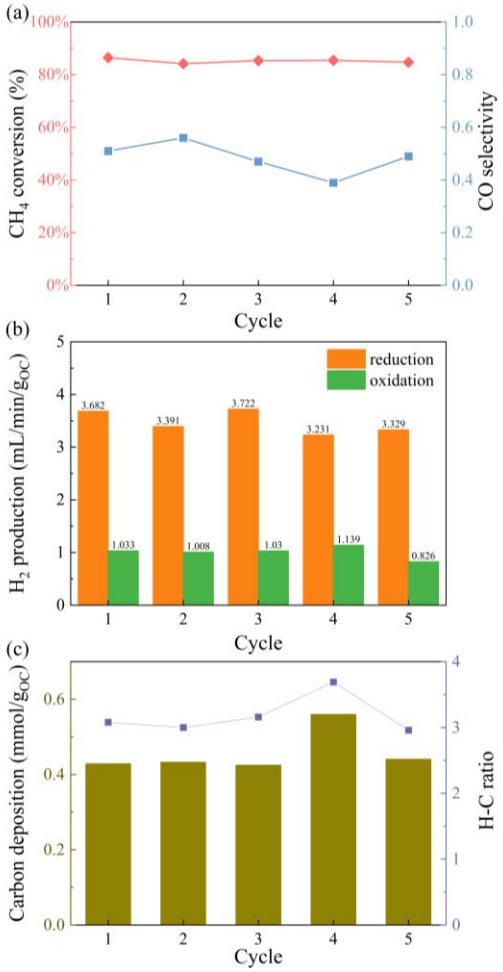

Fig. 5. The oxygen carrier particles behavior during the chemical looping reaction, (a) CH_4 conversion and CO selectivity, (b) H_2 yield in the two stages of reduction and oxidation, (c) carbon deposition and H-C ratio.

3.3 Effect of reaction temperature

We studied the reaction performance of the oxygen carrier particles in a wide range of operating temperatures. As shown in Fig. 6, the reaction performance of both CH_4 conversion and H_2 production throughout the cycle universally increases nearly linearly with temperatures between 450°C and 600°C. More than 60% CH_4 conversion can be achieved above 525°C. Especially, 85% CH_4 conversion can be achieved at 600°C. As the temperature decreases, the decline in H_2 production gradually increases. The possible reason is that in the medium-low temperature, the main reaction in the reduction stage is the methane steam reforming under the catalysis of Ni, and the participation of Fe-based oxygen carriers decreases.

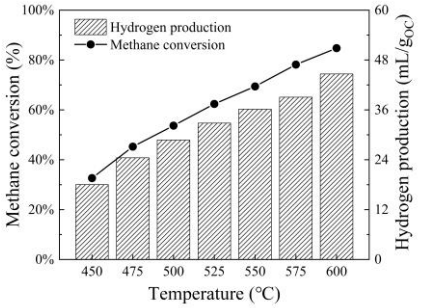

Fig. 6. Reaction performance of the oxygen carrier particles at different temperatures.

3.4 *Cycle stability*

To test the cycle stability of the oxygen carrier particles at 600°C, 20 redox cycles were carried out in the fixed reactor and 150 cycles were carried out in TGA. From Fig. 7a, the conversion rate of CH_4 is stable at 85-90%, and the H_2 production in the whole cycle is stable at 11-12 ml, indicating that the reaction performance is very stable over 20 cycles.

XRD patterns for the fresh Fe-P and reaction cycled Fe-P are shown in Fig. 7b. Since water vapor is used as the reaction gas in the oxidation step, the valence state of iron can only be restored to ferric oxide, and nickel can't be oxidized. The crystal phase results after reaction are Fe_3O_4 and Ni which are consistent with the prediction. The stability of the crystalline phase structure is confirmed by the clarity of the diffraction peaks after multiple cycles.

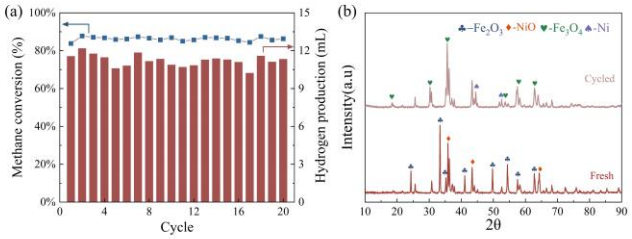

Fig. 7. (a) Reaction performance of 20 cycles under the condition that CH_4 reduction for 5 min and H_2O oxidation for 10 min, (b) XRD patterns of Fe-based particles

What's more, the weight loss curve of 150 cycles in which the weight loss had no obvious fluctuation indicates that the formed particles are very stable under multiple cycles as shown in Fig. 8. The results indicate that even after hundreds of cycles, the formed particles still have stable reactivity while maintaining high mechanical strength.

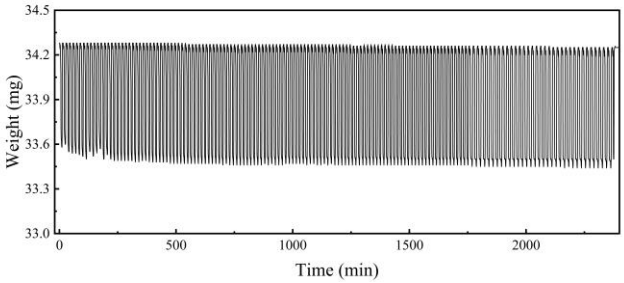

Fig. 8. Weight loss curve of 150 cycles monitored by TGA at 600°C under the condition that CH_4 reduction for 5 min and Air oxidation for 4 min.

4. CONCLUSIONS

In this study, we employed two metal oxide particles, namely nickel-based (Ni-P) and iron-based (Fe-P), as oxygen carriers. By mixing these two types of oxygen carrier particles, the chemical looping reaction of methane steam reforming participated by Fe-based oxygen carrier at 600°C was realized. Experiments with mixed particles and non-mixed particles revealed that the mixture of particles can promote the hydrogen production and methane conversion compared with non-mixed particles. Notably, the optimal mass ratio between Ni-based particles and Fe-based particles was found to be 1:3.

The results of physical characterization indicated that the particles exhibited exceptional mechanical strength, with no significant decrease observed. The methane conversion remained stable at about 87%, and the oxidation stage could achieve a 35% hydrogen production rate to the reduction stage. Furthermore, the thermogravimetric analysis results indicated that the oxygen gain and loss capacity remained relatively consistent with negligible fluctuations. In conclusion, our works provide oxygen carrier particles with a relatively simple preparation method to achieve chemical looping hydrogen production, which will have an impact on large-scale oxygen carrier preparation and chemical looping demonstration applications.

ACKNOWLEDGEMENT

The authors would like to acknowledge the support by National Natural Science Foundation of China (NSFC) (Grant No. 52241601 and No.52176026).

DECLARATION OF INTEREST STATEMENT

The authors declare that they have no known competing financial interests or personal relationships that could have appeared to influence the work reported in this paper. All authors read and approved the final manuscript.

REFERENCE

[1] Cozzi L, Gould T, Bouckart S, Crow D, Kim T, Mcglade C, et al. World energy outlook 2020. International Energy Agency: Paris, France. 2020:1-461.

[2] Cao Y, Zhang H, Liu X, Jiang Q, Hong H. A strategy of mid-temperature natural gas based chemical looping reforming for hydrogen production. International Journal of Hydrogen Energy. 2022;47:12052-66.

[3] Siriwardane R, Tian HJ, Fisher J. Production of pure hydrogen and synthesis gas with Cu-Fe oxygen carriers using combined processes of chemical looping combustion and methane decomposition/reforming. International Journal of Hydrogen Energy. 2015;40:1698-708.

[4] Zhu X, Wang H, Wei YG, Li KZ, Cheng XM. Reaction characteristics of chemical-looping steam methane reforming over a Ce-ZrO2 solid solution oxygen carrier. Mendeleev Communications. 2011;21:221-3.

[5] Jiang QQ, Zhang H, Cao YL, Hong H, Jin HG. Solar hydrogen production via perovskite-based chemical-looping steam methane reforming. Energy Conversion and Management. 2019;187:523-36.

[6] Wang J, Li K, Wang H, Li Z, Zhu X. Sandwich Ni-phyllosilicate@doped-ceria for moderate-temperature chemical looping dry reforming of methane. Fuel Processing Technology. 2022;232.

[7] Hu J, Chen S, Xiang W. Ni, Co and Cu-promoted iron-based oxygen carriers in methane-fueled chemical looping hydrogen generation process. Fuel Processing Technology. 2021;221.

[8] Qin L, Guo M, Liu Y, Cheng Z, Fan JA, Fan L-S. Enhanced methane conversion in chemical looping partial

oxidation systems using a copper doping modification. Applied Catalysis B: Environmental. 2018;235:143-9.
[9] Luo M, Yi Y, Wang SZ, Wang ZL, Du M, Pan JF, et al. Review of hydrogen production using chemical-looping technology. Renewable & Sustainable Energy Reviews. 2018;81:3186-214.
[10] Chen C, Chen C-H, Chang M-H, Lee H-H, Chang Y-C, Wen T-W, et al. A 30-kWth moving-bed chemical looping system for hydrogen production. International Journal of Greenhouse Gas Control. 2020;95:102954.
[11] Ma JC, Tian X, Wang CQ, Chen X, Zhao HB. Performance of a 50 kW(th) coal-fuelled chemical looping combustor. International Journal of Greenhouse Gas Control. 2018;75:98-106.
[12] Wei GQ, He F, Huang Z, Zheng AQ, Zhao K, Li HB. Continuous Operation of a 10 kW(th) Chemical Looping Integrated Fluidized Bed Reactor for Gasifying Biomass Using an Iron-Based Oxygen Carrier. Energy & Fuels. 2015;29:233-41.
[13] Hsieh TL, Xu DK, Zhang YT, Nadgouda S, Wang DW, Chung C, et al. 250 kW(th) high pressure pilot demonstration of the syngas chemical looping system for high purity H-2 production with CO2 capture. Applied Energy. 2018;230:1660-72.
[14] Haider SK, Azimi G, Duan L, Anthony EJ, Patchigolla K, Oakey JE, et al. Enhancing properties of iron and manganese ores as oxygen carriers for chemical looping processes by dry impregnation. Applied Energy. 2016;163:41-50.
[15] Pans MA, Gayan P, Abad A, Garcia-Labiano F, de Diego LF, Adanez J. Use of chemically and physically mixed iron and nickel oxides as oxygen carriers for gas combustion in a CLC process. Fuel Processing Technology. 2013;115:152-63.
[16] Steinfeld A, Kuhn P, Karni J. High-temperature solar thermochemistry: Production of iron and synthesis gas by Fe3O4-reduction with methane. Energy. 1993;18:239-49.
[17] Liu S, He F, Huang Z, Zheng A, Feng Y, Shen Y, et al. Screening of NiFe2O4 Nanoparticles as Oxygen Carrier in Chemical Looping Hydrogen Production. Energy & Fuels. 2016;30:4251-62.
[18] Medrano JA, Hamers HP, Williams G, Annaland MV, Gallucci F. NiO/CaAl2O4 as active oxygen carrier for low temperature chemical looping applications. Applied Energy. 2015;158:86-96.
[19] Liu MK, Zhang JR, Yang TL, Rao Q, Gai ZR, Zhao JX, et al. Light-enhanced thermochemical production of solar fuels from methane via nickel-based redox cycle. Fuel. 2023;335.
[20] Linderholm C, Mattisson T, Lyngfelt A. Long-term integrity testing of spray-dried particles in a 10-kW chemical-looping combustor using natural gas as fuel. Fuel. 2009;88:2083-96.
[21] Markstrom P, Linderholm C, Lyngfelt A. Chemical-looping combustion of solid fuels - Design and operation of a 100 kW unit with bituminous coal. International Journal of Greenhouse Gas Control. 2013;15:150-62.
[22] Lim HS, Kang D, Lee JW. Phase transition of Fe2O3–NiO to NiFe2O4 in perovskite catalytic particles for enhanced methane chemical looping reforming-decomposition with CO2 conversion. Applied Catalysis B: Environmental. 2017;202:175-83.